

Supporting Information

Qualitative and quantitative detection and identification of two benzodiazepines based on SERS and convolutional neural network technology

Xuanyu Sha^a, Guoqiang Fang^a, Guangxu Cao^b, Shuzhi Li^c, Wuliji Hasi^{a,†}, Siqingaowa Han^{c,†}

^aNational Key Laboratory of Science and Technology on Tunable Laser, Harbin Institute of Technology, Harbin, 150080, P. R. China.

^bResearch Center for Space Control and Inertial Technology, Harbin Institute of Technology, Harbin, 150080, P. R. China.

^cAffiliated Hospital of Inner Mongolia University for the Nationalities, Tongliao, 028043, P. R. China.

E-mail address: hasiwuliji@126.com

hansiqin@126.com

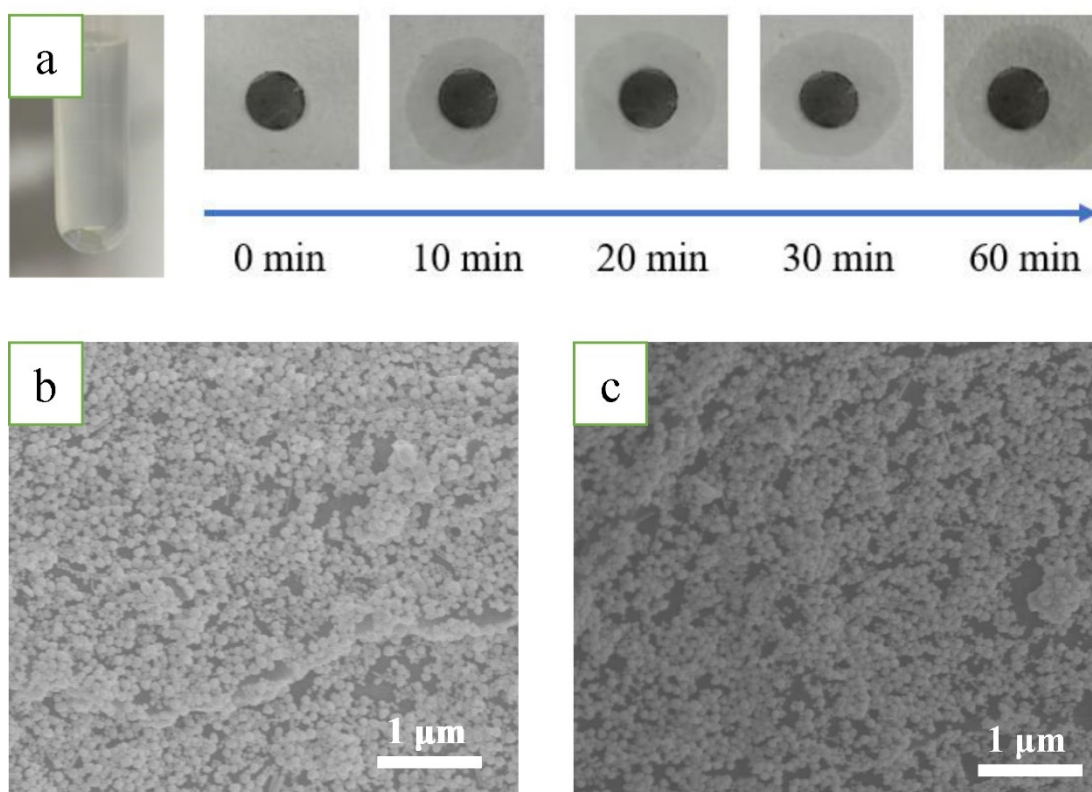


Fig. S1. (a) Picture of filter paper substrate after soaking. (b) SEM of nanoparticles assembled on the surface of paper-based fibers before soaking. (c) SEM of nanoparticles assembled on the surface of paper-based fibers after soaking.

It should be noted that the assembled filter paper SERS substrate should be used after drying, and cannot be directly immersed in the solution to be tested.

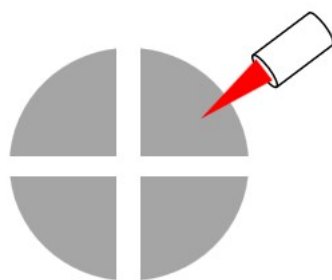


Fig. S2. Quartered filter paper substrate for spectral acquisition

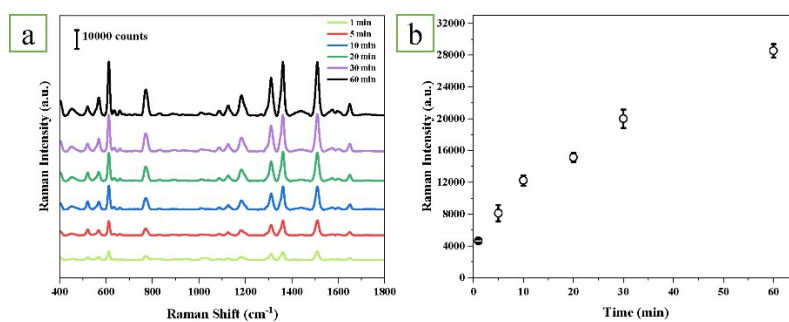


Fig. S3. (a) Variation of the paper-based SERS spectral intensity of probe R6G (500 ppb) under different soaking times, (b) the change of characteristic peak intensity (1508 cm^{-1}) with soaking time of paper-based SERS substrate relation chart.

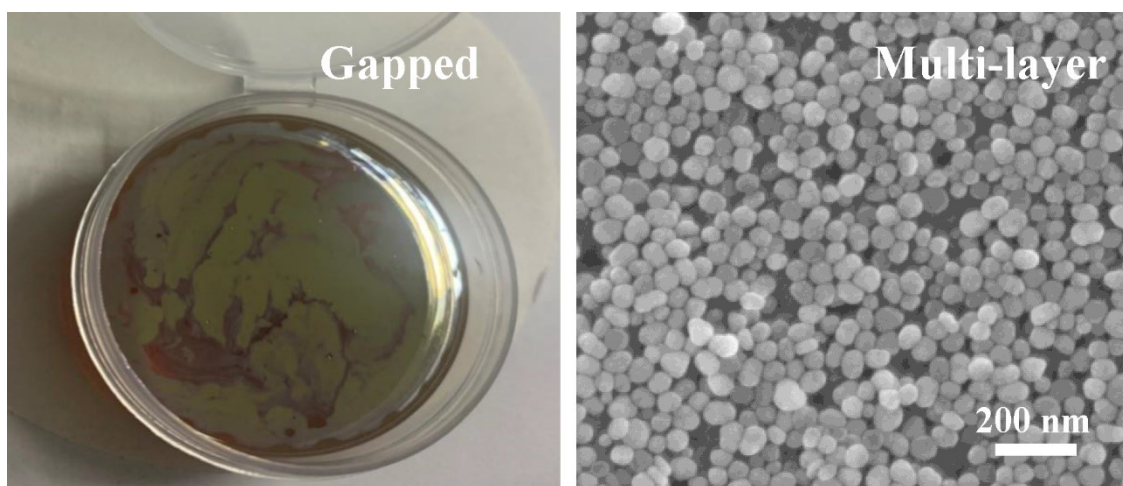


Fig. S4. Characterization of SERS substrates assembled by traditional two-phase self-assemble method a) Macro view of a silver film with gaps b) SEM of silver nanoparticles assembled on wafer.

Table S1. Vibrational mode assignment of midazolam Raman characteristic peaks

Theoretical calculation (cm ⁻¹)	SERS spectrum (cm ⁻¹)	Ascription
692	689	Def(Ring)
834	826	Ring breathing
1049	1035	Def(Ring)
1302	1301	v(ph)
1562	1562	v(ph), v(C-C)
1600	1611	v(C-N), v(C-C)

Notation: def = deformation, v = stretching; δ = bending; γ = out-of-plane deformation; ph = Phenyl.

Table S2. Vibrational mode assignment of diazepam Raman characteristic peaks

Theoretical calculation (cm ⁻¹)	SERS spectrum (cm ⁻¹)	Ascription
689	689	Def(Ring)
989	976	Ring breathing
	998	
1031	1026	δ (C-H)
1168	1178	v(C-C-N)
1333	1325	v(C-C), δ (C-H)
1400	1392	v(C-C)
1568	1555	v(C-C)
1614	1594	v(C-N), v(C-C)
1644	1625	v(C-O), v(C-N), v(C-C)

Notation: def = deformation, v = stretching; δ = bending; γ = out-of-plane deformation; ph = Phenyl.

Enhancement factor calculation

The analytical enhancement factor of the prepared filter paper substrate was studied. The calculation formula is as follows:

$$AEF = \frac{I_{SERS}}{I_{RS}} \times \frac{C_{RS}}{C_{SERS}}$$

Where I_{SERS} and I_{RS} are the SERS signal intensity (41407 counts) of R6G molecules on the surface of the filter paper substrate and the conventional Raman signal intensity (631 counts) of R6G aqueous solution, respectively. C_{SERS} and C_{RS} are corresponded to the tested sample concentrations in SERS (1 ppm) and conventional Raman spectra (10^3 ppm), respectively. The calculated AEF was 6.56×10^4 for Ag assembled filter paper substrate.

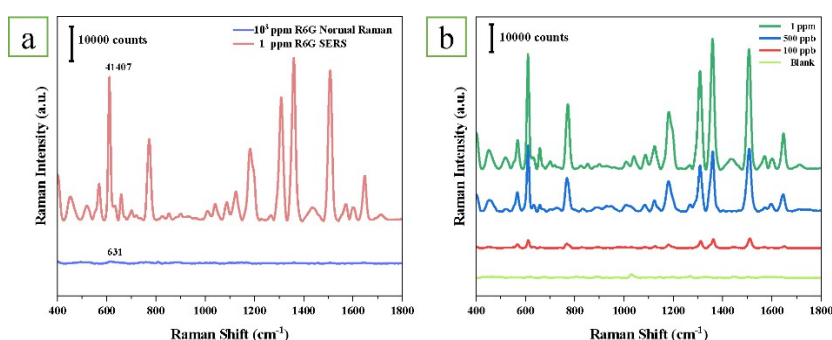


Fig.S5. (a) Comparison of conventional Raman signal intensity Raman spectrum(10^3 ppm) and SERS spectrum(1 ppm) intensity of R6G probe detected by paper-based SERS substrate (b) SERS spectra of gradient concentrations of R6G.

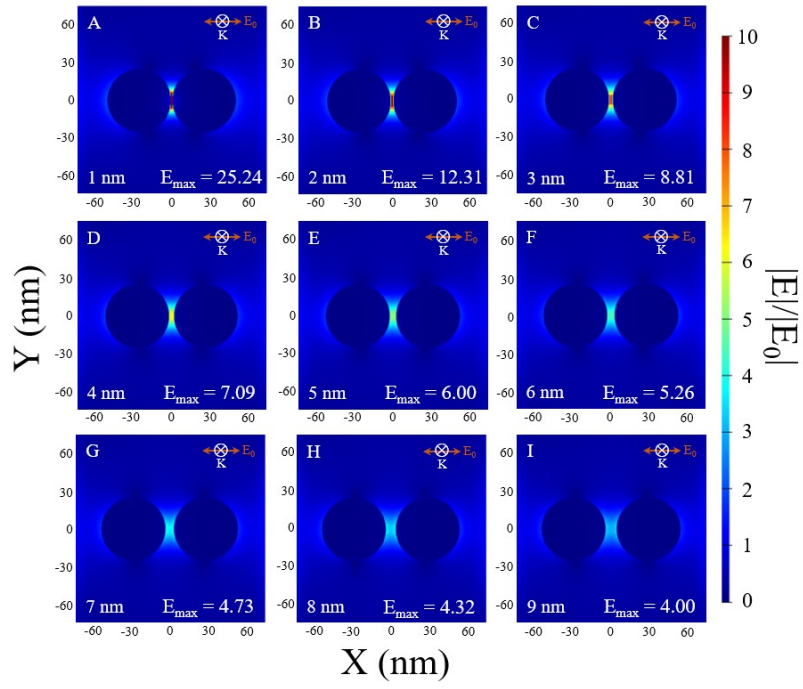


Fig.S6 The local electric field intensity distribution between silver nanospheres (50-50 nm) at different spacing (1~9 nm)

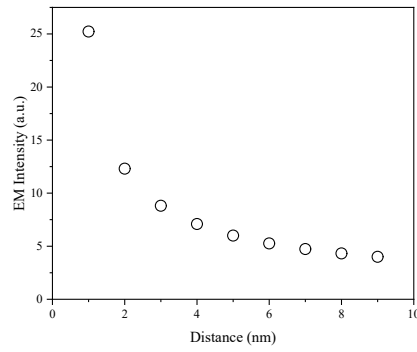


Fig.S7 Local electric field intensity between silver nanosphere with different spacing (1~9 nm)

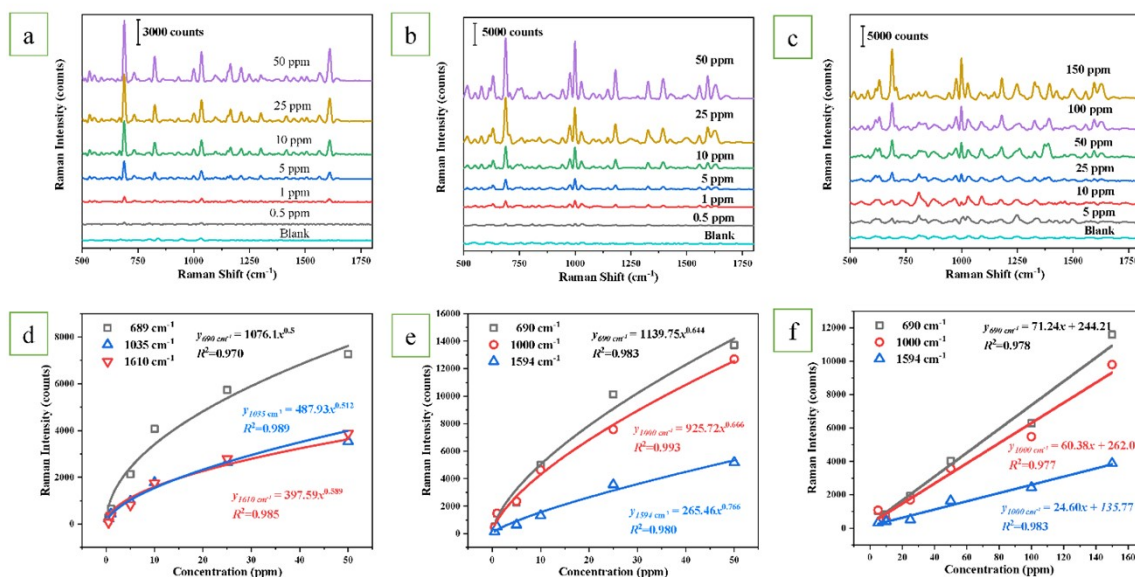


Fig.S8. (a) SERS spectra of midazolam Sprite samples with gradient concentrations; (b) SERS spectra of diazepam aqueous samples with gradient concentrations; (c) SERS spectra of diazepam Sprite samples with gradient concentrations. (d) the relationship between midazolam Sprite sample concentrations and Raman intensity of characteristic peak at 689, 1035, 1610 cm⁻¹; (e) the relationship between diazepam aqueous sample concentrations and Raman intensity of characteristic peak at 690, 1000, 1594 cm⁻¹; (f) the relationship between diazepam Sprite sample concentrations and Raman intensity of characteristic peak at 690, 1000, 1594 cm⁻¹.

Table S3. Detailed concentration distribution for 560 spectra

Concentration(ppm)	Midazolam in water	Midazolam in Sprite	Diazepam in water	Diazepam in Sprite
0.1	15	-	-	-
0.5	15	20	20	-
1	15	20	20	-
2.5	15	-	-	-
5	15	20	20	20
10	15	20	20	20
25	15	20	20	20
50	15	20	20	20
100	-	-	-	20
150	-	-	-	20
Total	120	120	120	120

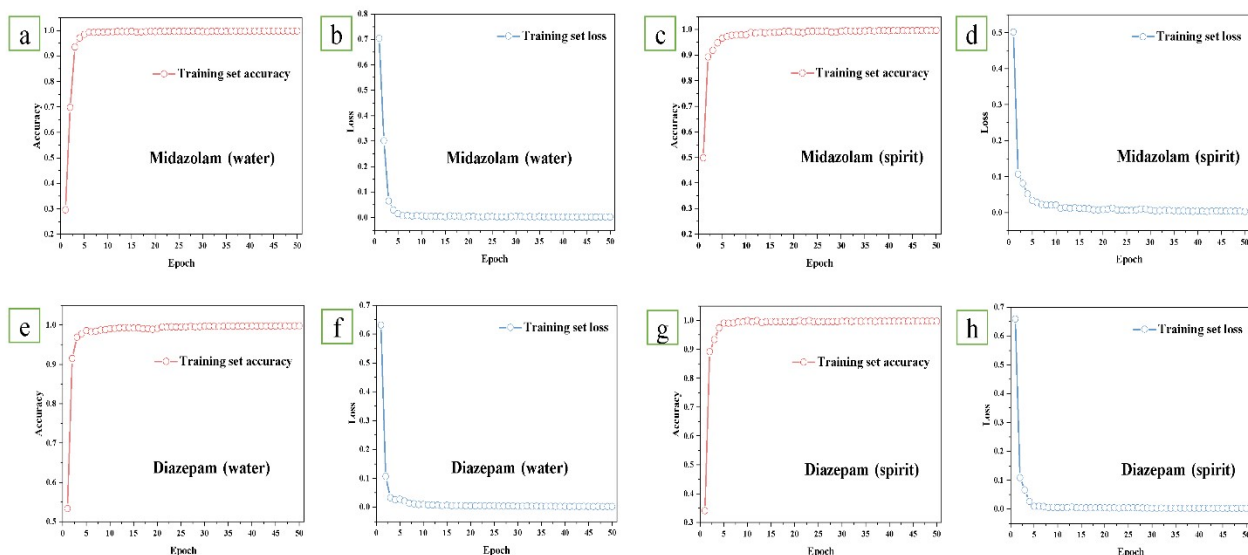


Fig. S9. Performance of CNN quantitative models. a) Accuracy for tested midazolam aqueous sample test set during model training, b) The loss value of optimized model for midazolam aqueous sample after each epoch. c) Accuracy for tested midazolam Spirit sample test set during model training, d) The loss value of optimized model for midazolam Spirit sample after each epoch. e) Accuracy for tested diazepam aqueous sample test set during model training, f) The loss value of optimized model for diazepam aqueous sample after each epoch. g) Accuracy for tested diazepam aqueous sample test set during model training, h) The loss value of optimized model for diazepam aqueous sample after each epoch.